Vol. 63: 171–190, 2015
doi: 10.3354/cr01291

CLIMATE RESEARCH
Clim Res

Published online May 20

Snowfall event characteristics from a high-elevation site in the Southern Appalachian Mountains, USA

Daniel T. Martin[1], L. Baker Perry[1,*], Douglas K. Miller[2], Peter T. Soulé[1]

[1]Department of Geography and Planning, Appalachian State University, Rankin Science West, 572 Rivers Street, Boone, NC 28608, USA

[2]Department of Atmospheric Sciences, University of North Carolina at Asheville, Robinson Hall, Asheville, NC 28804, USA

ABSTRACT: Accurate assessment of snowfall patterns in high-elevation remote areas is essential to providing a foundation for further climatological analyses. The Southern Appalachian Mountain (SAM) region of the eastern US provides a unique study area due to its low latitude and proximity to the Gulf of Mexico and Atlantic Ocean. Major snowstorms, such as the remnants of Hurricane Sandy in October 2012, can result in heavy snowfall of 100 cm or greater in favorable upslope regions. Understanding the behavior of these precipitation patterns is important due to flooding threats caused by a combination of factors including deep snowpack exposed to heavy rainfall, cloud immersion, and high dew point temperatures, further exacerbating flooding threats. To contribute to this understanding, we installed the Mobile Precipitation Research and Monitoring (MOPRAM) station at Roan Mountain (1875 m) on the Tennessee/North Carolina border in October 2012. MOPRAM allowed us to analyze liquid equivalent precipitation, new snowfall, snow depth, air temperature, and relative humidity at high temporal resolutions during the 2012–2013 snow season. We present the observed snowfall event characteristics (e.g. new snowfall, liquid equivalent precipitation, atmospheric conditions, and synoptic patterns) along with how these characteristics compare to other sites in the SAM. In our 25 event dataset, we observed the following patterns: conditionally unstable upstream lapse rates; predominantly northwest winds; high-to-low elevation precipitation enhancement near a factor of 3; and 364 mm of snow liquid equivalent on Roan Mountain. An estimated 391 cm of snow fell at Roan during the 2012–2013 season using nearby snow liquid ratios as an estimate for snowfall.

KEY WORDS: Orographic snowfall · New snowfall properties · Southern Appalachian Mountains

1. INTRODUCTION

The dynamic multiscale forcings governing snowfall rates and amounts in mountainous terrain can be especially difficult for forecasters and climatologists to diagnose due to complex interactions between physical barriers and a poorly observed atmosphere. What sampling does exist suffers complications from instrumentation challenges, especially when measuring snowfall (Rasmussen et al. 2012). Because the spatial scale of mountain influences is often very fine — on the order of kilometers or less — current atmospheric models cannot easily resolve precipitation patterns for a wide variety of snowfall regimes such as synoptically driven flows (e.g. Miller-style systems) or mesoscale-forced flows (e.g. upslope precipitation). At the climatological level, understanding how these fine spatial patterns are reacting to climatic shifts is important for predicting the outcome of many important hydrological resources. While comprehensive studies of mountain meteorology such as the Mesoscale Alpine Programme (MAP) have made

*Corresponding author: perrylb@appstate.edu

important contributions (Medina et al. 2005), the atmospheric processes and patterns in mountainous areas remain poorly understood because of low population densities and associated limited observational networks due to inaccessible locations when compared to valley, coastal, or plains regions (Barry 2008).

One reason the Southern Appalachian Mountain (SAM) region of the US serves as a unique test bed for the analysis of snowfall climatology is the high frequency of events at higher elevations from a variety of synoptic regimes, such as Gulf and Atlantic lows, 500 hPa cutoff lows, and Alberta Clippers (Perry et al. 2010). Additionally, this region is characterized by considerable topographic relief leading to high spatial variability of precipitation. The most extreme of these spatial gradients is associated with northwest flow snowfall (NWFS), which is often characterized by orographically enhanced precipitation on northwest slopes in the wake of synoptic-scale subsidence behind a surface cold front (Perry 2006). With an elevation range between 183 and 2037 m, the SAM region has the greatest topographic relief in the eastern US. Key features of this domain include the southeast-facing Blue Ridge Escarpment in North Carolina (NC), the Great Smoky Mountains National Park (GSMNP) and Unaka Range on the borders of NC and Tennessee, and the Black Mountains of NC, home to Mount Mitchell, the highest point east of the Mississippi River (2037 m). Annual average snowfall in the region can range from <10 cm in the southeast foothills to >250 cm in high-elevation windward escarpment regions such as Mt. LeConte in the GSMNP (Perry & Konrad 2006).

This dramatic spatial variability makes the SAM a unique region in the southeastern US when compared to Piedmont regions with substantially more uniform climate patterns. Consequently, understanding of meteorological processes in the SAM remains an integral part of the culture for both the support of tourism and the prevention and assessment of natural hazards. The 755 km Blue Ridge Parkway spans from north-central Virginia to the GSMNP in western NC. In 2012, over 17 million visitors travelled the Parkway primarily for recreation (National Park Service 2012). This extensive road network extends to elevations over 1850 m in the western portion and as a result is subject to frequent closures due to snow and ice (Meyers 2006).

While the ski resorts of the western US boast greater acreage, trail lengths, and vertical ascents, the SAM has remained an important winter recreation destination for citizens of the East due to its nearby location and reliable winter weather climatology (Johnson 1987). While not dependent on natural snowfall due to a high capacity for snowmaking, cold weather and natural snow enhance the experience and often lead to larger crowds on the slopes. Additionally, the presence of perennial snow cover in remote areas such as Roan Mountain and along the Blue Ridge Parkway often provides an environment conducive for cross-country skiing that attracts visitors.

The diverse terrain and climate of the SAM also make possible a number of natural hazards such as flooding, landslides, and potent winter storms. In 2004, torrential rainfall, attributed to the remnants of Hurricanes Frances and Ivan, triggered multiple landslides claiming 5 lives and 16 homes (Wooten et al. 2008). In 1998, deadly flooding affected the town of Roan Mountain; this was ultimately associated with the combination of heavy rainfall and melting of the existing deep snowpack on Roan Mountain (1916 m), and resulted in 7 fatalities (Hunter & Boyd 1999). While such natural phenomena cannot be prevented, the appropriate warning and response can be enhanced through effective study and understanding of orographic precipitation regimes in the region.

Observation networks in the SAM such as the Cooperative Observer (COOP) and NC Environment and Climate Observation Network (ECONet) have grown in recent years (Holder et al. 2006). However, automated representation of favorable upslope snowfall sites remains lacking. To address this lack of sites, we installed the Mobile Precipitation Research and Monitoring (MOPRAM) station on Roan Mountain just south of the Tennessee border (elevation ~1875 m) on 30 September 2012 (Fig. 1). We chose Roan Mountain for 2 primary reasons. First, the combination of elevation and exposure results in frequent snowfall events from multiple storm tracks (Johnson 1987). Second, the site has no known climatological observations at the summit (nearby COOP sites are ~1000 m or more lower in elevation). The MOPRAM station now provides hourly observations of temperature, relative humidity, liquid precipitation, and snow depth within a sparsely instrumented region.

We present results from the first year of MOPRAM data, exploring in detail lesser understood contributors to snowfall in the SAM such as lapse rates, wind direction, and antecedent air trajectories. Characteristics rarely sampled in the SAM such as orographic enhancement, lee drying, and event-scale variability are of particular interest, and are addressed in our analysis. In addition, we explore 2 case studies in

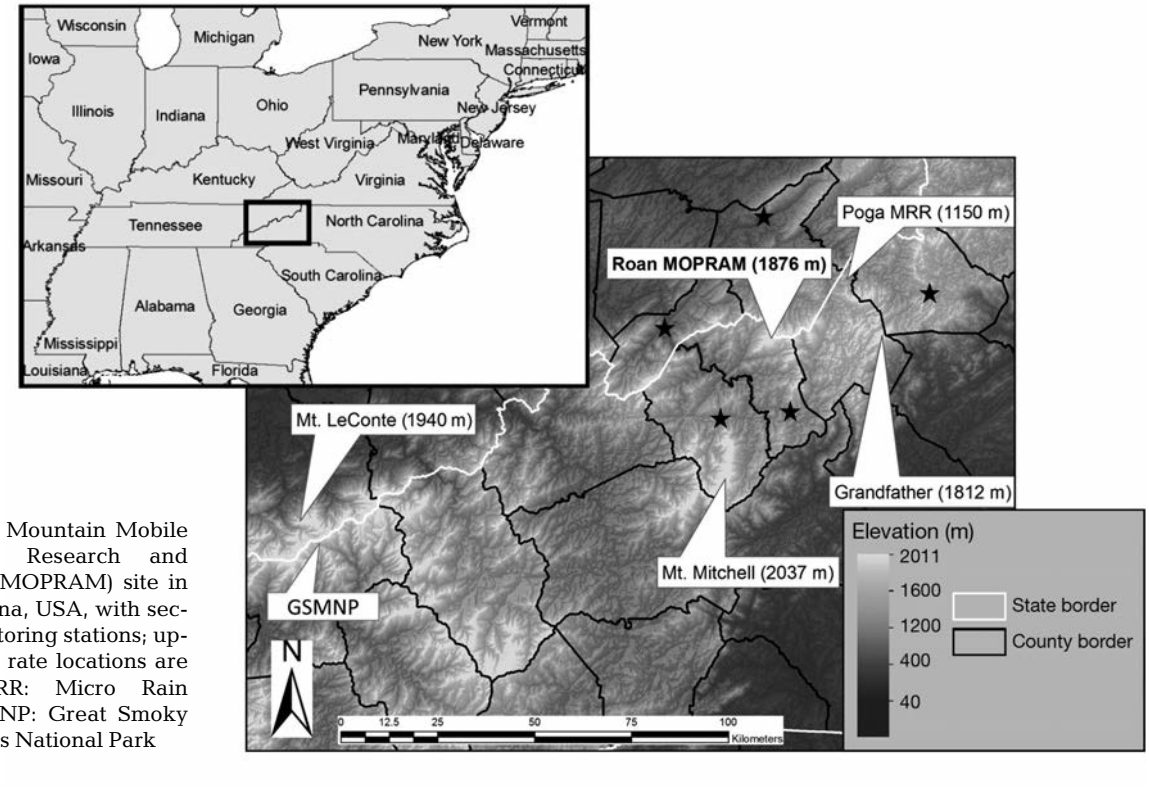

Fig. 1. Roan Mountain Mobile Precipitation Research and Monitoring (MOPRAM) site in North Carolina, USA, with secondary monitoring stations; upstream lapse rate locations are starred. MRR: Micro Rain Radar; GSMNP: Great Smoky Mountains National Park

detail — the remnants of Hurricane Sandy and a prolonged late-March snowstorm — in order to analyze the atmospheric processes and associated snowfall patterns involved with events having relatively high societal impacts. The research project was largely motivated by the inter-event mesoscale variability of snowfall and associated atmospheric processes that often result in heavy snowfall on the higher elevation windward slopes and only trace amounts at downwind locations.

Our guiding research questions were:

(1) What atmospheric variables most influence snowfall event characteristics at high-elevation sites in the SAM, and how do these characteristics vary at the event scale (e.g. liquid equivalent, snowfall, lapse rates)?

(2) What synoptic patterns (e.g. Miller cyclones, Alberta Clippers) produced the bulk of the snowfall and snow liquid equivalent during the winter of 2012–2013?

(3) How do these different patterns modulate lee phenomena (e.g. lee drying, spillover) at the event scale?

(4) How do snowfall and snow depth on Roan Mountain compare with other high-elevation COOP stations located above 1800 m (e.g. Mt. LeConte, Mt. Mitchell)?

2. BACKGROUND

2.1. Observations of snowfall in mountainous regions

Mountain regions are characterized in part by pronounced variability of temperature, precipitation, wind, and other parameters over small spatial scales (Barry 2008). However, most weather stations are located in valley regions and the density of observations in mountain regions is generally low. In the US, the challenge of poor mountain observation density has to some extent been mitigated in recent years with the development of volunteer networks such as the Community Collaborative Rain Hail and Snow Network (Cifelli et al. 2005, Doesken 2007) and the National Weather Service (NWS) COOP program, the growth of which has been overtaken by state-level climate programs such as the NC ECONet. This instrumentation suite has complemented the existing COOP and Automated Surface Observing System/Automated Weather Observing System station network and compares quite well with the COOP temperature and precipitation observations (Holder et al. 2006). Where gaps still exist in datasets, model interpolation projects such as the Parameter-elevation Relationships on Independent Slopes Model (PRISM,

Daly et al. 2008) have used known relationships of orography and nearby stations to create continuous grids of approximate precipitation values. While precipitation typically increases with elevation up to a certain point, the degree to which this effect occurs can vary greatly by region, synoptic regime, and mountain feature (Basist et al. 1994).

Despite advances in mountain observation and density, such as miniaturized equipment, solar panels, and telemetry (Barry 2008), observing precipitation — especially snowfall — still remains a challenge. Factors such as the phase change of snowfall (e.g. melting, sublimation), as well as the physical redistribution of accumulations by wind, are strong hindrances to properly assessing accumulation amounts; settling and compaction of fresh snowfall over time can also produce varying totals as a function of observation hour (Doesken & Leffler 2000). Undercatch of precipitation gauges also remains a problem, as light ice crystals are wind-driven away from collection sites, creating substantial error in snow liquid equivalent amounts. Rasmussen et al. (2012) assessed various configurations of snow gauges with results suggesting that great improvement in measurement can be found with those gauges surrounded by alter shields and fences or surrounded by dense bushes or forest, though these are not always practical due to limited space and cost. Attempts to model and potentially correct for blowing and drifting snow have also been explored to better explain the redistribution of snow in open environments (Gauer 1998).

If adequate calibrations are in place, snow depth can also be measured by automatic acoustic methods with an accuracy of up to 1 cm (e.g. see http://s.campbellsci.com/documents/us/manuals/sr50a.pdf). However, errors can be introduced as a function of snow density — low-density snow, as a poor reflector of sound, is more difficult to accurately assess than existing/compacted snowpack. Using derived snow totals, these sonic snow depth sensors can accurately measure new snowfall in some cases, especially when derived at high temporal resolutions and when settling and compaction are taken into account (Ryan et al. 2008).

2.2. Snowfall patterns in the SAM

Snowfall in the SAM is driven by a variety of synoptic and mesoscale processes depending on low-level wind direction. Northwestern slopes (e.g. Great Smoky Mountains and Unaka Mountains) see a majority of their snowfall from NWFS events, those characterized by the orographic enhancement of snowfall in association with low-level northwest (270 to 360°) flow (Perry 2006). This northwest flow typically follows the cold frontal passage of Miller cyclones — mid-latitude cyclones that can be categorized either Miller A, originating in the Gulf of Mexico and traversing across the Atlantic seaboard, or Miller B, originating in the Ohio Valley with secondary cyclogenesis along the Atlantic seaboard (Miller 1946). Eastern escarpments such as the Blue Ridge, however, see most of their snowfall from gulf lows as well as cold air damming (CAD) events, during which a surface ridge in the northeastern US wedges cold air against the mountains and allows isentropic lift in the eastern mountains and Piedmont of NC and Virginia while maintaining sub-freezing wet bulb temperatures near the surface (Bell & Bosart 1988). Although previous work (e.g. Perry 2006, Keighton et al. 2009) has suggested that the majority of the snowfall at higher elevations and along northwestern slopes is associated with low-level northwest flow, our analysis of detailed event-level observations in this study aims to more fully investigate the mesoscale variability and the atmospheric processes.

Focus has been on NWFS due to its high spatial variability, wide latitudinal distribution in the Appalachians, and potential to produce heavy snowfall amounts. Collaborations between NWS offices and select universities continue to address the problems with NWFS forecasting while contributing to a growing climatology of synoptic snowfall event types (Keighton et al. 2009). Through these collaborations, we have found that a variety of influences such as moisture fluxes from the Great Lakes (Holloway 2007), ground heat and moisture fluxes (Miller 2012), and parcel trajectory (Perry et al. 2007) impact snowfall totals. In particular, these analyses suggest that trajectories with a Great Lakes connection can enhance snowfall totals, which is consistent with the findings of Alcott & Steenburgh (2013) that show that moisture fluxes from upstream sources such as lakes can significantly contribute to snowfall totals in mountain regions.

3.0. DATA AND METHODS

3.1. Roan Mountain MOPRAM

The MOPRAM station on Roan Mountain includes an OTT Pluvio^2 weighing precipitation gauge (resolution ± 0.1 mm) which has a good track record of accuracy (Sevruk et al. 2009). Additionally, we used

Table 1. Data sources for short-term snowfall climatology at Roan Mountain, North Carolina, USA

Variable(s)	Elevation (m) or location	Temporal resolution	Source
Temperature and relative humidity	1875	1 min	Vaisala HMP45C probe
Grandfather Mountain wind speed and direction	1609	1 min	RM Young 05103 Alpine
Liquid equivalent precipitation	1875	1 min	Pluvio weighing gauge
SYNOP present weather code[a]	1875	1 min	Parsivel disdrometer
Radar reflectivity and Doppler velocity	1018	1 min	Micro Rain Radar (MRR)
Surface analyses	United States	3 h	NOAA Weather Prediction Center
New snowfall, snow liquid equivalent, and density	1875	12 h	Manual observations
Gauge-collected total precipitation	1018	12 h	Manual observations

[a]Unavailable after 7 November 2012

its associated alter wind shield, OTT Parsivel^2 disdrometer and present weather sensor, Campbell Scientific CR1000 datalogger, sonic snow depth sensor (resolution ± 1 cm), soil moisture and soil temperature sensors, solar radiation sensor, temperature and relative humidity sensor, and photovoltaic power supply and battery (Table 1). The MOPRAM station site is located in a clearing surrounded by red spruce *Picea rubens* Sarg. and Fraser fir *Abies fraseri* Pursh trees, providing an optimal site for minimizing wind effects on precipitation measurements and snow accumulation. Unfortunately, low sun angles in late autumn, frequent storms, and associated cloud cover and snow accumulation on the solar array led to the failure of the separate battery for the OTT Parsivel^2 after just 2 events in November 2012. However, the remaining sensors, including the Pluvio^2 weighing precipitation gauge and sonic snow depth sensor, continued to operate on a separate power supply. Therefore, for this study, the Pluvio^2 was used to identify precipitation events.

3.2. Wind and radar data

In addition to the Roan Mountain MOPRAM site, a suite of instrumentation on nearby but lower sites allowed us to obtain additional meteorological data for each snowfall event. For the purposes of synoptic-scale wind and echo height determination, the geographic displacement of these stations from the Roan Mountain site (Fig. 1) is relatively small, allowing for a reasonable comparison of variables not available at the Roan Mountain study site. Wind data were collected from RM Young Alpine 05103-45 propeller anemometers on 10 m towers atop Poga Mountain (1140 m) and Grandfather Mountain (1609 m). A vertically pointing Micro Rain Radar (MRR) (Peters et. al 2002) was deployed at 1018 m on Poga Mountain (25 km northeast of Roan) to further contribute to both precipitation type estimation via hydrometeor Doppler velocity (e.g. Yuter et al. 2008) and investigation of the vertical structure of snow events (Stark et al. 2013).

3.3. Trajectory analyses

Using the HYSPLIT EDAS 40 km trajectory model (Draxler & Rolph 1998), we analyzed backward parcel trajectories ending at Roan Mountain (1875 m). By integrating these trajectories back 72 h, we could determine antecedent upstream air trajectories, with particular interest in trajectories featuring a Great Lakes connection. Using a previously delineated series of domains (Fig. 2, modified from Perry et al. 2007), we calculated the amount of time each trajec-

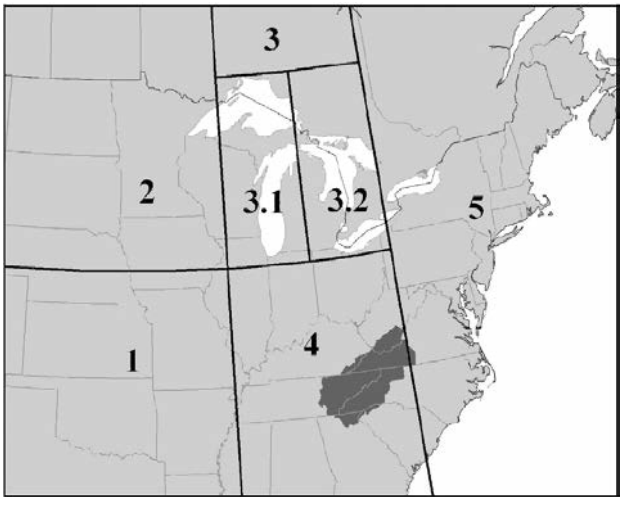

Fig. 2. Sub-domains for HYSPLIT trajectory analyses (Southern Appalachian Mountains are shaded dark gray). Modified from Perry et al. (2007)

tory spent in the individual sub-domains during the previous 72 h in order to test the hypothesis that a Great Lakes moisture flux can enhance snowfall totals (e.g. Holloway 2007). An additional calculation demanded that an antecedent parcel reside in both Great Lakes regions for at least 6 h each (for a 12 h total minimum Great Lakes influence).

3.4. Snowfall event categorization

We determined the time-frame for the snow events using a multi-parameter approach combining hourly observations of snow water equivalent (SWE), precipitation, temperature, snow depth, and echo top height/MRR Doppler velocities. The beginning of an event was determined by the first hour when solid precipitation >0.25 mm was observed; the maturation hour was the hour of heaviest precipitation as measured by the Pluvio^2, and ending at the last hour of recorded solid precipitation. An event remained active as long as measurable solid precipitation was reported during a 6 h period; breaks over 6 h resulted in the identification of separate snowfall events. Because the present weather sensor was not operational during the latter part of the study, we identified snowfall events on the basis of (1) SWE >0 in conjunction with surface temperatures <2°C, and (2) total event snow depth >1 cm as observed by the sonic snow depth sensor. We chose 2°C, as previous studies have demonstrated that this is often the upper threshold at which solid precipitation is observed (e.g. Yuter et al. 2006).

Melting layer heights were determined using an automated algorithm in the NCSU OPL Viewer Software (North Carolina State University Department of Marine, Earth and Atmospheric Sciences, Cloud and Precipitation Processes and Patterns Group). The automated algorithm looks for the largest vertical gradient in both Z (level Z) and Doppler velocity (level W). If those heights agree within 3 gates (i.e. both see the gradient in almost the same place), the height is computed using (level Z + level W +1)/2. Otherwise, if the algorithm does not see a strong gradient or if the heights from W and Z do not agree, the melting layer height is not plotted. We corroborated the automated method using a qualitative approach — we searched rather obvious increases in fall speeds which were indicative of a snow to liquid transition. We also used a qualitative approach to determine melting layer height in the event the OPL MRR software did not have sufficient data. To further delineate precipitation types at Roan Mountain without the help of a disdrometer, we used a quasi-objective methodology: sub-freezing precipitation hours showing no snow depth change were typically classified as freezing rain, although a manual case-by-case analysis using MRR velocity data determined whether snow was also possible (Yuter et al. 2008). These mixed precipitation events that likely minimized snow accumulation were rather common, necessitating the corroboration of other parameters. By using a combination of reflectivity and velocity, we could determine snowfall (rainfall) levels by identifying the level at which lower (higher) reflectivity and fall speeds existed.

3.5. Derivation of snowfall event statistics

Upon identification of individual snowfall events, we explored statistical characteristics from both raw (e.g. temperature, relative humidity, snow depth) and derived (e.g. event-level snowfall, lapse rates, orographic enhancement) data. We classified the synoptic-scale circulation associated with each snow event according to a modified version (Perry et al. 2013) of the Perry et al. (2010) manual scheme developed for an analysis of snowfall events in the Great Smoky Mountain region of the SAM (Table 2). We derived lapse rates using the height differential between an upstream station and Roan Mountain (Fig. 1) and analyzed at the event level to explore the degree of instability within each snowfall period. The chosen up-

Table 2. Synoptic event classifications. From Perry et al. (2013)

Class	Description
NE-U	Northeastward tracking low passes to the north of area
SE-U	Southeastward tracking clipper that passes north or across the area
M-U	Miller A/B cyclones originating in the Gulf of Mexico
CL-U	Cutoff low — a 500 hPa cutoff low moves across region (often slow and sometimes quasi-stationary)
LC-U	Lee cyclogenesis — surface lows develop to the lee of the Appalachian Mountains
U	Upslope — W/NW upslope flow in the absence of synoptic-scale surface features
Non-U	Non-NW flow events
X-U	Unclassified — does not fit any of the synoptic classes
*-U	Denotes upslope flow (250 to 360°) at event maturation for any of the synoptic classes

wind stations were those whose directions from Roan matched most closely the direction of recorded wind at the event maturation hour. Temperatures at event maturation were used to further investigate the low-level temperature profile just upwind of Roan Mountain. The orographic enhancement factor was also calculated as the ratio of Roan SWE to Poga event total SWE. We used identical weighing precipitation gauges (i.e. Pluvio^2) with single alter shields in relatively sheltered locations in this calculation, increasing the confidence in the comparisons.

We considered and delineated precipitation type into rain, snow, and freezing rain; we also analyzed the precipitation events and intensity according to time of day (12:00 to 00:00 h UTC and 00:00 to 12:00 h UTC, respectively) to determine whether snowfall displays any unusual behavior during the overnight hours as suggested by Miller (2012). The addition of freezing rain for the study site was warranted after a sufficient number of hours showed substantial sub-freezing precipitation accumulation with little-to-no snow accumulation reported by the acoustic snow depth sensor. The method for seasonal snowfall estimation incorporated known snow liquid ratios (SLRs) for concurrent events by using the sum of SWE reported at Roan and the reported SLR at Poga Mountain, the product of which would be a fair estimator for snowfall. In the case of an event yielding only rain and/or negligible snowfall at Poga Mountain, a 'warm SLR' of 5:1 (200 kg m^{-3}) was applied to the corresponding Roan Mountain total to provide a conservative estimate of the snowfall.

4. RESULTS

4.1. Summary statistics

We found that during the 2012–2013 snow season from 1 October 2012 to 31 May 2013, 25 snowfall events occurred at Roan that were suitable for further study due to storm total accumulation being >1 cm (Table 3). Event dates ranged from 28 October 2012 to 4 April 2013. Event lengths varied, with event durations ranging 1 to 69 h from first recorded precipitation to a 6 h lull. Events of higher length were attributed to prolonged northwest flow snowfall, with the longest duration belonging to the remnants of Hurricane Sandy. Total SWE also varied within events, the catalogue in total seeing 353 mm with event minima of 2 mm and maxima of 79 mm, the latter being attributed to Sandy as well.

Table 3. Summary statistics (N = 25) for 2012–2013 snowfall event categorizations at Roan Mountain, North Carolina, USA

	Duration (h)	Snow water equivalent (mm)	Snowfall (cm)	Temperature (°C)	Relative humidity (%)
Total	472	353	391		
Mean	19	14	16	−6.7	93.5
Min	1	2	1	−15.4	83.6
Max	69	79	80	2.4	100

4.2. Wind direction and radar

Wind direction histograms sampling the 472 event hours showed a strong northwest tendency for nearby Poga Mountain and Grandfather Mountain sites (Fig. 3a), indicative of the post-frontal nature of many of the snow events witnessed during the 2012–2013 season. Seventy-one percent (336 event hours) of wind records at Poga Mountain during snowfall events were between 270 and 360°, with a small secondary maximum of easterly winds. Grandfather Mountain saw a similar dominance in northwesterly winds, with wind directions between 270 and 360° observed during 67% (319) of event hours. Exploring a connection between wind direction and precipitation intensity, we categorized the percentage of event hours into light (<1 mm h^{-1}), moderate (1 mm h^{-1} < liquid precipitation < 3 mm h^{-1}), and heavy (>3 mm h^{-1}) precipitation and found that precipitation followed the same directional trends, with a slight shift south and westward for the heaviest events (Fig. 3b).

Our radar analysis of the events showed that echo top heights and melting layer heights typically decrease from beginning to end of events (Table 4). However, this change is dependent on synoptic class, with all of the events that are characterized by northwest flow (U; see Table 2) at event maturation exhibiting a decrease in echo top height as the subsidence inversion strengthens and lowers and a reduction in melting layer heights in association with lower tropospheric cold advection (e.g. Perry et al. 2007). With other shorter duration events dominated by isentropic lift and no northwest flow, little change in echo top heights is noted. Whereas high echo tops (>5650 m) were observed for 25% of event beginning hours, this value dropped dramatically for maturation hours (8.7%) to 0% for ending hours. By contrast, few event beginning hours (3%) saw echo

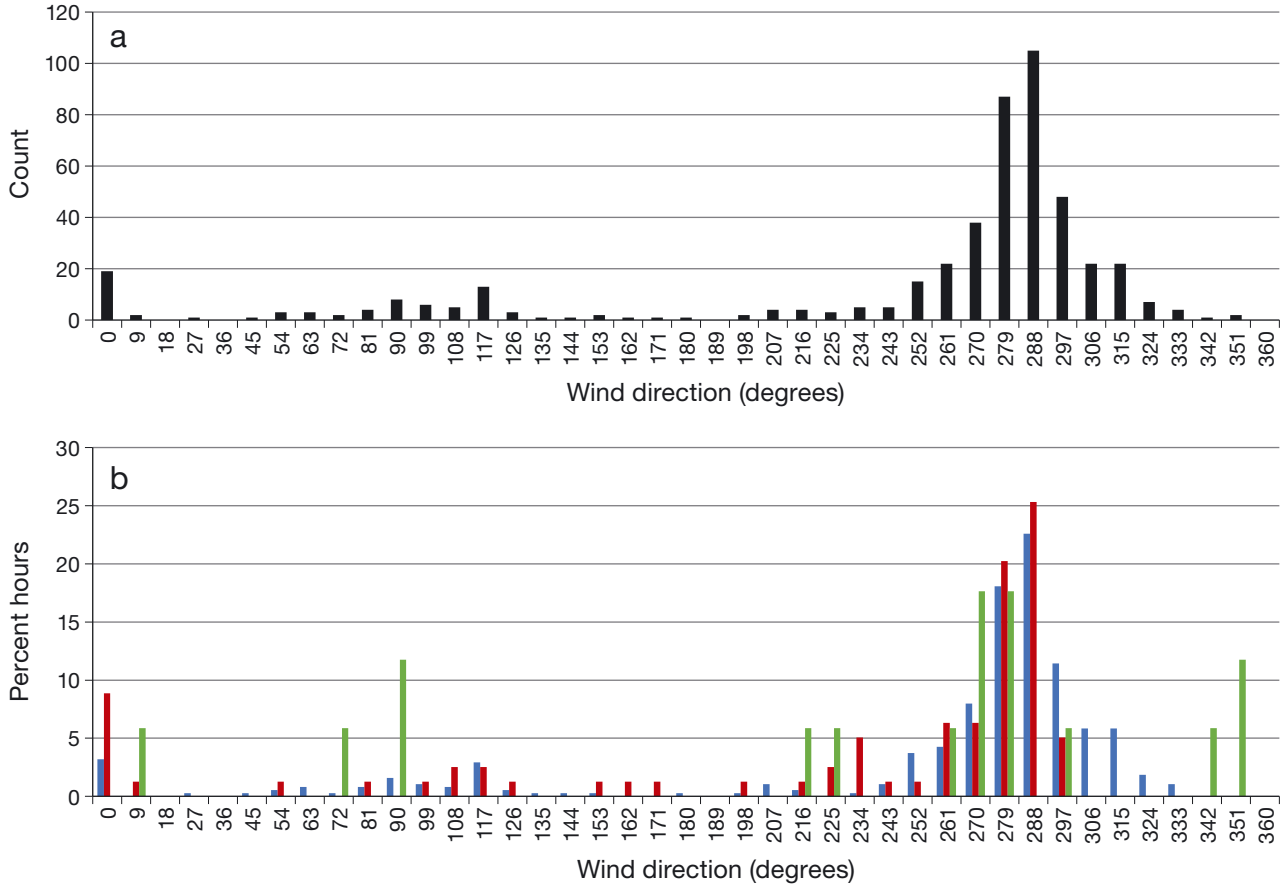

Fig. 3. (a) Wind frequency for all snowfall event hours for the 2012–2013 snowfall season at Poga Mountain, North Carolina (USA) and (b) percentage hours by precipitation intensity (blue: light; red: moderate; green: heavy)

Table 4. Summary statistics for Micro Rain Radar event echo top and melting heights

	Echo tops (m)			Melting height (m)		
	Begin	Maturation	End	Begin	Maturation	End
Mean	3433	3102	2166	1479	1376	1358
Max	5650	5650	4150	2950	2950	2950
Min	1450	1750	1450	Surface	Surface	Surface

tops <2500 m, while over a third (36.8%) saw these shallow values by the event ending hour.

4.3. Trajectory analyses

Antecedent air parcels resided inside domain 4 (Ohio River Valley, see Fig. 2) for over half of all trajectory hours (Table 5). Additionally, domain 1 (southwest) held 25.9% of antecedent parcel trajectory hours. A small amount of parcel residence occurred in the Great Lakes domains during the 2012–2013 season, with only ~5% of total event hours seen in these regions. When binning hours according to the classification scheme of Perry et al. (2007), we noted that 3 events (12% of total) were influenced by antecedent trajectories with a Great Lakes influence (i.e. parcel residence times >6 h in both Great Lakes domains). The longest residence time in the Great Lakes domains (31 h) was attributed to a 10 h precipitation event during mid-February 2013 where only 5 mm of liquid equivalent precipitation fell.

4.4. Statistics by synoptic event class

Although summary statistics delineated by synoptic event type (Table 2) show a dominance of Miller cyclones, it is important to recognize that these findings are for a single winter season and may not necessarily be representative of a longer-term climatology. The prevalence of this synoptic type is contrasted with a

Table 5. HYSPLIT 72 h antecedent air trajectory characteristics for snowfall events. GLC: Great Lakes connection

Class	% Events	No.	Description
1	20	5	≥36 h in region 1, no GLC
2	8	2	≥36 h in region 2, no GLC
3.1	8	2	≥6 h in W Great Lakes
3.2	8	2	≥6 h in E Great Lakes
3.3	4	1	≥6 h in W and E Great Lakes
4	40	10	≥36 h in region 4, no GLC, <36 h in either regions 1 or 2
5	12	3	Remainder
		25	Total

Table 6. Snowfall event characteristics at Roan Mountain, North Carolina, USA, by synoptic class (see Table 2 for a description of synoptic classes). SWE: snow water equivalent

Synoptic class	Percent of events	Percent of snowfall	Percent of SWE	Duration (h)	Snowfall (cm)	SWE (mm)
NE-U	8	3	5	25	11	17
SE-U	12	20	16	36	63	57
M-U	24	39	21	145	116	74
CL-U	0	0	0	0	0	0
LC-U	0	0	0	0	0	0
U	12	12	2	91	25	9
Non-U	32	22	41	86	88	145
X-U	12	3	16	89	88	57

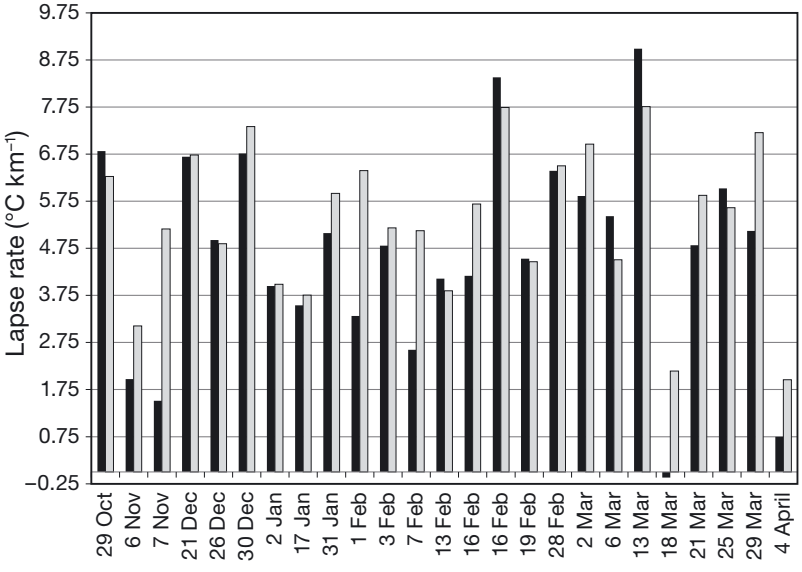

Fig. 4. Derived event maturation lapse rates by event number between upstream stations and Roan Mountain (black) and average of all stations (grey) for 2012–2013 snowfall season in the Southern Appalachian Mountains

total absence of cutoff lows (Table 6). While the greatest number of events were classified as non-U (0 < maturation and wind direction < 250), the greatest contribution by hours and SWE was attributed to Miller events. While non-NWFS events contributed less than a third of events, they contributed the highest total of SWE (41%) and consisted primarily of Miller events. The large contribution of X-U events was attributed to the Sandy remnants, as only 1 other tropical cyclone (Hurricane Ginny, 1963) may have resulted in snowfall in the southern Appalachian Mountains since 1950 (L.G. Lee pers. comm.). The lowest observed wind speeds by synoptic event class were during a non-NWFS Miller event in early March, with a maturation wind speed of <1 m s^{-1} recorded at both stations. However, on average, Miller systems had the highest event wind speeds with an average of 36 knots; the outlier occurred on 7 November 2012 when light winds at maturation hour could be associated with a secondary upper-level low to the west cancelling out any northerly flow from the main system. It should be noted that these wind speeds may at times have been under-represented due to the frequent presence of riming at our sites, although any biases were kept relatively low, with an average difference of 0.87 m s^{-1} for the events sampled between the unheated propeller anemometers used in this study and a Vaisala WS425 FG heated sonic anemometer available for part of the snow season on Grandfather Mountain.

4.5. Lapse rates

Upstream horizontally estimated lapse rates (Γ) for the 2012–2013 snowfall season ranged from −0.1 to 9.0°C km^{-1}, with a seasonal event maturation average of 4.7°C km^{-1} (Fig. 4). Additionally, it is important to note that the lower troposphere for 7 of the 25 events was conditionally unstable (6 < Γ < 9.8°C km^{-1}). This finding should be taken into consideration as the degree of instability that can allow for discrete, cellular snow squalls to be embedded within the larger-scale NWFS (Miller 2012); this phenomenon was noticeable

at times on the MRR profiles. Only 1 event saw an inverted lapse rate at its maturation hour, indicative of an inversion layer typically seen with a CAD scenario (Bell & Bosart 1988). Lapse rate findings are consistent with the synoptic cold air advection regime characterizing a majority of the snowfall hours. Agreement between the chosen upwind site and the average of all sites for the event series was particularly high (r = 0.82).

4.6. Orographic enhancement

With the exception of a few outliers, the ratio of Roan to Poga Mountain liquid equivalent precipitation totals was approximately 3 (mean 3.2, Fig. 5). Nine events were not categorized due to a lack of reported concurrent precipitation at both the Roan and Poga Mountain sites. With enhancement ranging from 0.95 to 3.75, no particular pattern was observed with respect to the higher/lower enhancement ratios when considering the synoptic classifications overall. One of the lowest values (1.13) was in association with the mid-January rain-to-snow event which was classified as a non-NWFS Miller A/B; these low ratios can be attributed to the widespread, deep nature of the moisture layer evenly distributing precipitation. Conversely, the highest ratio (3.75) was in association with a mid-February cold front whose parent low (classified as an NE-U; see Table 2) was well to the north of the SAM. As is typical with NWFS events, the spatial gradients of precipitation were very high even for sites within kilometers of each other, due to isolated banding and orographic enhancement, therefore leading to the high difference in SWE between Roan and Poga Mountain. Other weak but notable patterns also emerged, including a weak negative correlation between orographic enhancement and lapse rate, as well as weak and moderate correlations between orographic enhancement and maturation wind speed and direction, respectively.

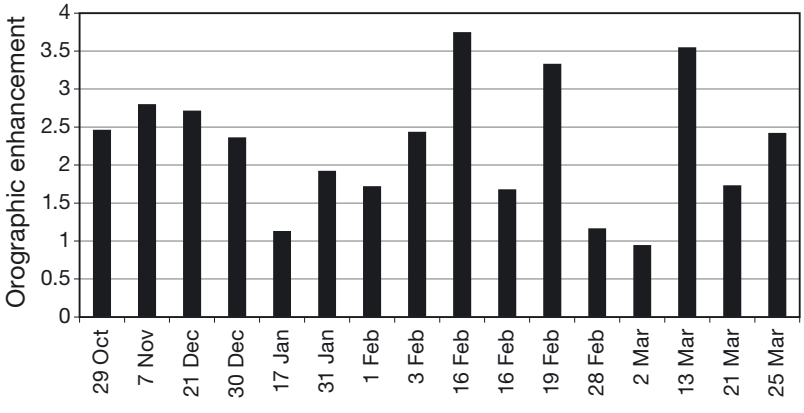

Fig. 5. Orographic enhancement ratios (ratio of Roan to Poga Mountains event total liquid precipitation) for snowfall events for the 2012–2013 season in the Southern Appalachian Mountains

4.7. Precipitation distribution by type

During the cold season (October–May), nearly half (49.5%) of all precipitation hours were classified as rain (Table 7); about a third of precipitation hours (33.2%) were in the form of snowfall, with the remainder (17.3%) falling as freezing rain. The active months of the season (JFM) had a similar distribution of precipitation type, though as expected frozen precipitation increased at the expense of liquid, yielding a nearly even 3-way split in contribution among the precipitation types. Additionally, no substantial difference between daytime and nighttime snowfall amounts was observed, each contributing approximately half of the season's liquid equivalent precipitation total. Manual observations of snowpack characteristics from 7 field visits throughout the season, highlighted the relatively consistent density of the snowpack (~200–300 kg m^3).

4.8. Seasonal snowfall trends

Snowfall during the 2012–2013 season at Roan Mountain was estimated at 391 cm, higher than the observations of several other high-elevation sites such as Mt. Mitchell (284 cm) and Mt. LeConte (327 cm). While these values indicate total snowfall slightly above the average annual snowfall for the most favored of windward escarpments (e.g. Mt. LeConte, mean annual snowfall of ~254 cm), it is important to consider that the Roan Mountain totals are derived from local SLRs, introducing a level of uncertainty in the station comparisons. Seasonal trends in snow depth indicated nearly continuous snow cover from late December through early April. Roan Mountain saw considerably more snow depth on the ground and duration of snow cover than Mt. Mitchell (Fig. 6), further highlighting the importance of exposure alongside elevation when considering the location of snowfall maxima. Also of note

Table 7. Distribution of seasonal precipitation by type and duration for Roan Mountain for the 2012–2013 snow season. SWE: snow water equivalent; U: upslope

Time period	Total precip (mm)	SWE Total (mm)	SWE %	SWE % Hours	Freezing rain Total (mm)	Freezing rain %	Freezing rain % Hours	Rain Total (mm)	Rain %	Rain % Hours
October–May	1350	353	26	33	144	11	17	854	63	50
January–March	655	222	34	38	122	19	26	310	47	35
Oct–May Day	721	182	52	53	100	70	52	439	52	49
Oct–May Night	630	171	48	47	44	30	47	414	48	51
U-only Day	135	135	54	51						
U-only Night	117	117	46	49						

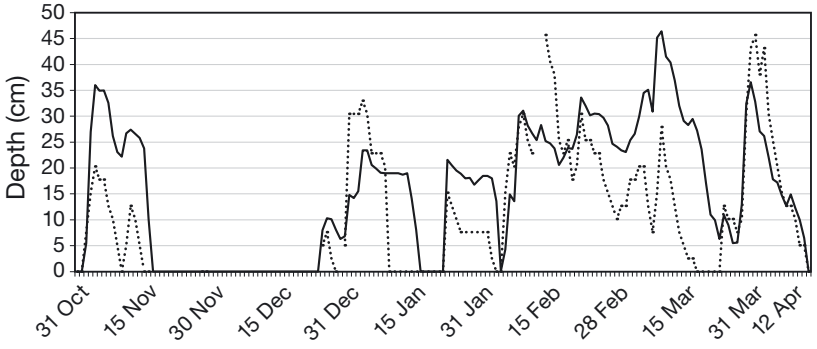

Fig. 6. Time series of snow depth from Roan Mountain (solid) and Mt. Mitchell (dotted), North Carolina, USA, for the 2012–2013 snowfall season

were several easterly-flow events during which Mitchell snow depth exceeded that recorded at Roan. Additionally, snow depth >1 cm (>25 cm) was recorded during 51% (18%) of all hours on Roan Mountain between 1 October 2012 and 31 May 2013. The snowy start to the season was balanced by lack of events and precipitation in the latter portion (April/May); no additional snow cover was observed at any station outside of the early April event. This translates to approximately 125 (43) d > 1 cm (>25 cm). Additionally, snow cover was present 66% of the time during DJF and 88% of the time during JFM.

4.9. Case studies

4.9.1. Hurricane Sandy

A late October 2012 storm was a rare interaction of a potent upper-level disturbance with the remnants of Hurricane Sandy (Galarneau et al. 2013). In addition to disastrous flooding on the east coast of the US, the storm's cold sector produced a substantial amount of snowfall in the SAM. This unusual snow event provided a unique case for the new instrumentation suite to record. A long wave mid-latitude trough phased with a tropical cyclone (Sandy) undergoing extratropical transition (Hart & Evans 2001) resulting in rapid cyclogenesis (Fig. 7) and strong and persistent northwest flow as the system passed to the northeast. The greatest values of liquid precipitation and snowfall of the season at Roan Mountain were also recorded (Fig. 8).

Precipitation from the remnants of Sandy began on 19:00 h UTC on 28 October as light rain that rapidly changed to snow, concurrent with strong cold air advection. As the only event recorded by the Parsivel^2 sensor, the delineation of particular precipitation types by hour was possible; 61 h of snow and 8 h of no precipitation were recorded during the event. By the event's end on 31 October, 79.5 mm of liquid equivalent precipitation had accumulated in the Pluvio^2 weighing precipitation gauge. This corresponds to at least 64 cm of snowfall using the 8:1 snowfall ratios manually recorded at nearby Poga Mountain. However, a site visit on 1 November 2012 measured 88 mm of SWE in the 70 cm of snow on the ground, indicating about an 8% undercatch by the Pluvio^2 weighing precipitation gauge, and considerable settling and compaction of the snowpack since the event began 4 d earlier. These values are comparable to the highest amounts reported by favorable upslope regions of the Appalachian Mountains, such as on Mt. LeConte and in the West Virginia Mountains. The storm was also characterized by high winds throughout the study region, although outside of some substantial high-elevation gusts, the majority of the wind damage remained in the New England states. Grandfather Mountain saw peak wind gusts of 47.3 m s^{-1}, although rime ice accumulation on the anemometer may have limited it from recording even higher values.

Radar characteristics of Sandy were similar to other heavy NWFS events. High initial echo top heights

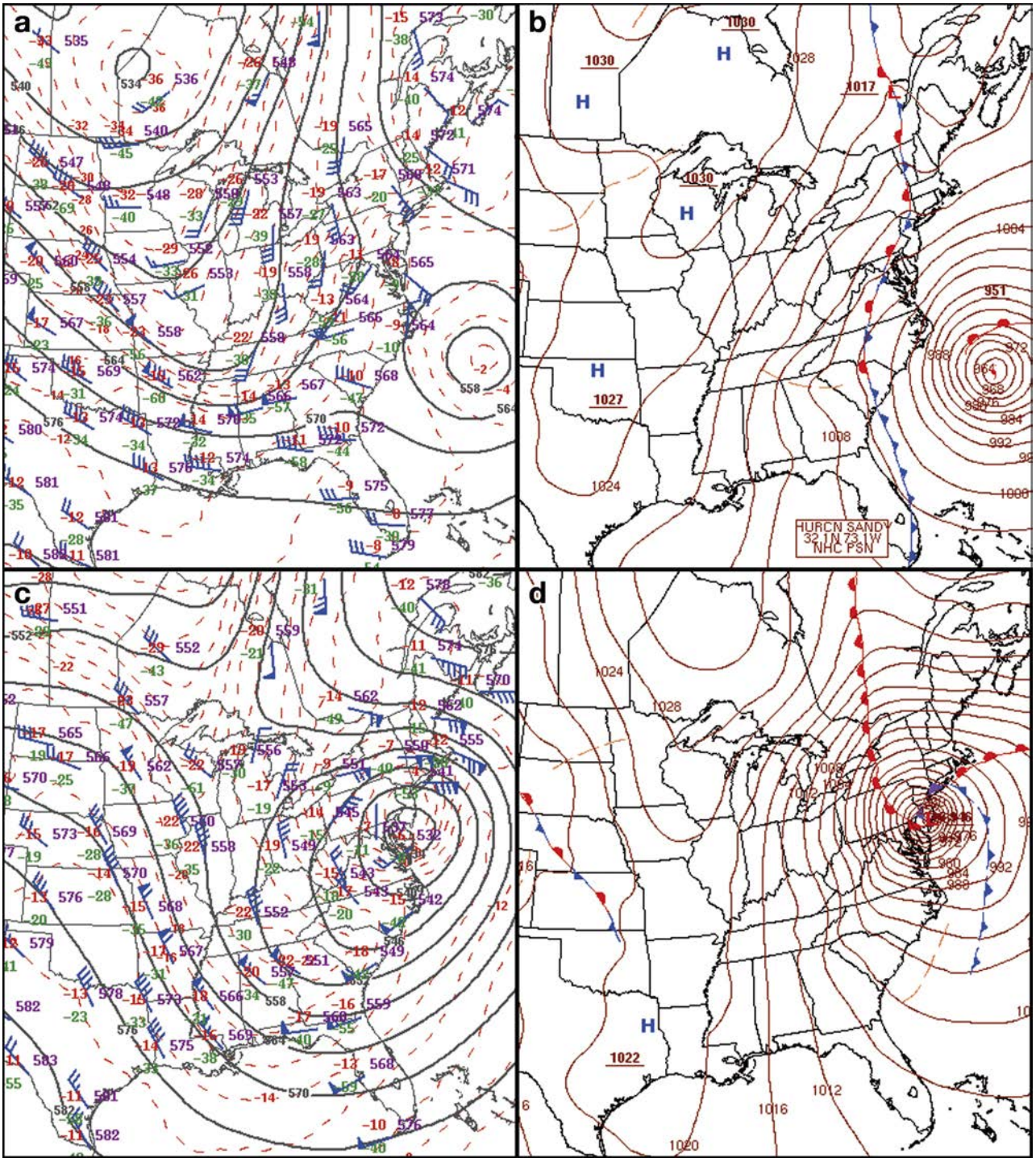

Fig. 7. NOAA Weather Prediction Center (WPC)-analyzed 500 hPa geopotential height (solid lines, dm), wind barbs (knots; 1 knot = 0.51 m s^{-1}) and temperature (dashed lines, °C) during Hurricane Sandy. (a) 12:00 h UTC on 28 October 2012 and (c) 00:00 h UTC on 30 October, and (b,d) WPC surface analysis for the same times (data source: www.spc.noaa.gov/obswx/maps). Purple: geopotential height (dm); red: temperature (°C); green: dewpoint temperature (°C)

(~4450 m) dropped to shallow levels (~2500 m) within hours of the beginning of the event. Hurricane Sandy provided a unique case study due to the fact that all of the ingredients necessary for a potent NWFS event were in place for a majority of the event: strong orthogonal winds, copious moisture support, and a

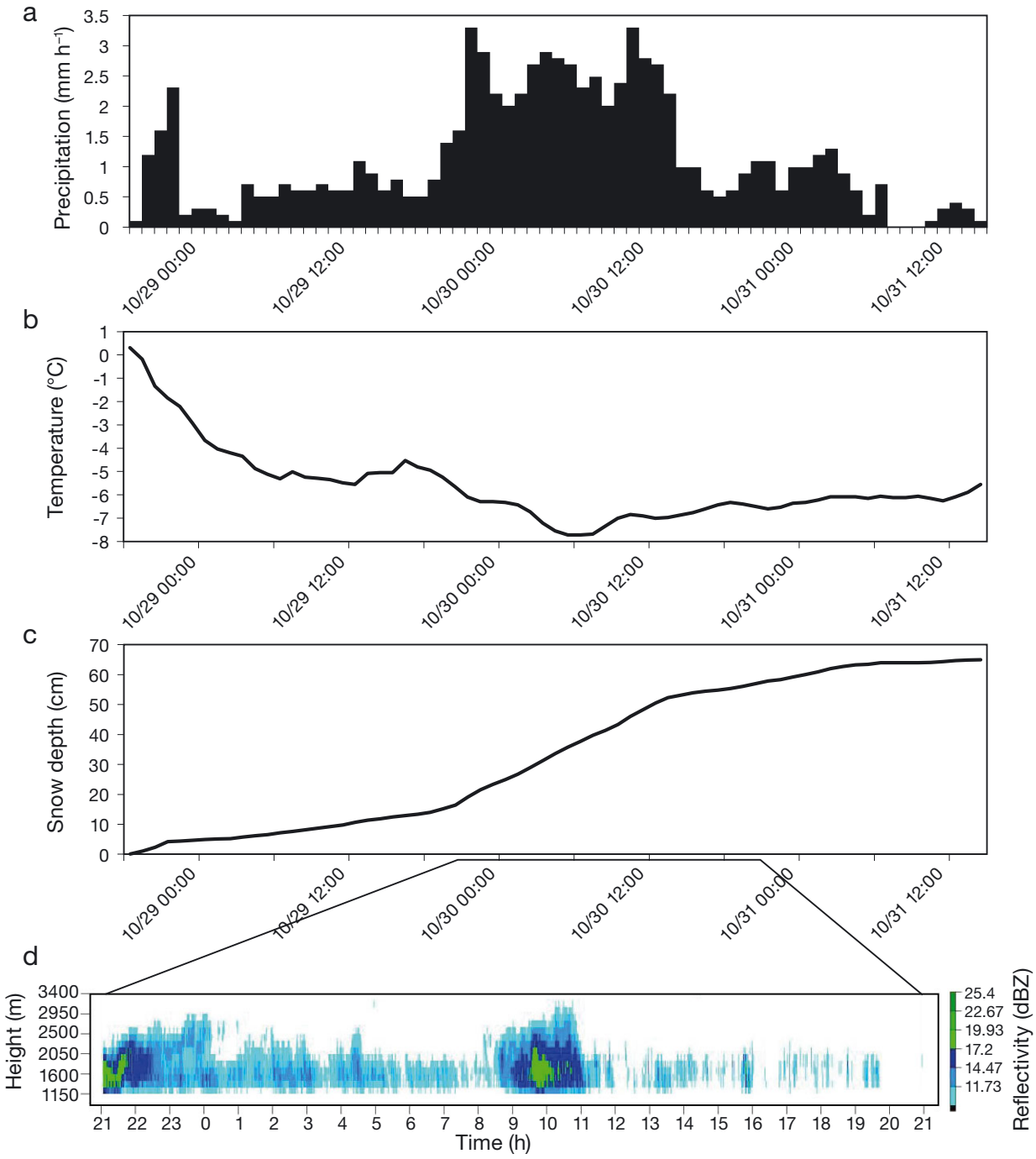

Fig. 8. (a) Hourly precipitation, (b) temperature, (c) cumulative snow depth, and (d) radar reflectivity for the 24 h period ending at 21:00 h UTC on 30 October for remnants of Hurricane Sandy (28–31 October 2012). Radar reflectivity images (d) created using NCSU (North Carolina State University) OPL Micro Rain Radar application version 0.9.0.75 (Prerelease), North Carolina State University Department of Marine, Earth and Atmospheric Sciences Cloud and Precipitation Processes and Patterns Group

slow-moving track. Trajectory analyses from both event hourly precipitation maxima (22:00 h UTC on 29 October, 11:00 h UTC on 30 October, Fig. 9) indicate not only a likely Atlantic Ocean moisture flux at the mid-levels (~700 hPa), but also a secondary Great Lakes flux due to the cyclonic rotation that existed at the lowest to middle levels (below 700 hPa); subfreezing temperatures at these moist layers also facilitated the development of dendritic snow growth, enhancing accumulations. Mid-level synoptic-scale

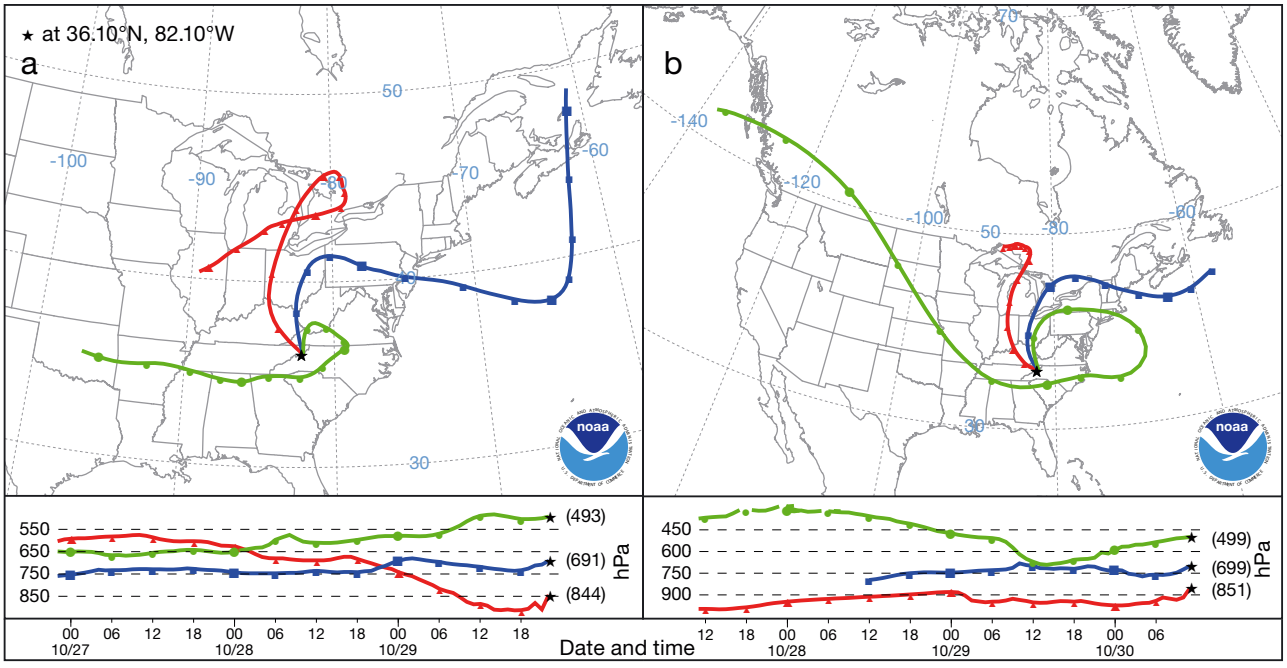

Fig. 9. 72 h antecedent air parcel trajectory originating at event precipitation maxima from snowfall episodes associated with remnants of Hurricane Sandy. (a) 22:00 h UTC on 29 October, (b) 11:00 h UTC on 30 October. Red, blue and green lines represent backward parcels ending at Roan Mountain (starred) at approximately 850, 700, and 500 hPa, respectively. Values in parentheses: pressure of the air parcel at the end of its trajectory

ascent allowed for a deeper moisture layer to develop, especially in the central Appalachians near the storm center. An additional mesoscale-level enhancement of precipitation totals can be attributed to the high winds providing a strong orographic component to snowfall development, even though the wind direction was less than optimal for truly mountain-orthogonal flow.

4.9.2. Late March prolonged NWFS

A second major snowstorm occurred in late March 2013 (Fig. 10), bringing in prolonged NWFS to the WNC region. A Miller A/B cyclone developed to the north and west of the study region on 25 March, with precipitation beginning shortly after midnight UTC; peak liquid precipitation rates shortly followed, exceeding 3.9 mm h^{-1} at the event maturation hour (06:00 h UTC 25 March, Fig. 11). The system slowly propagated northeastward, exposing the region to strong northwest winds, rapidly decreasing temperatures, and NWFS before the storm departed by 27 March 2013, leaving 44.3 mm SWE (estimated 55 cm of snowfall) on Roan. HYSPLIT trajectory analyses at the 2 precipitation maxima for the event (20:00 h UTC 25 March, 19:00 h UTC 26 March, Fig. 12) display that in contrast to Sandy's Atlantic moisture influence, Great Lakes fetch at the mid-to-upper pressure levels (~700–500 hPa) served as a primary provider of upstream moisture. Radar trends were typical of a NWFS event. After an initial series of high echo tops (~4400 m), synoptic-scale subsidence quickly set in, keeping tops around 2300 m outside of a short period of heavier snowfall which brought tops of 3000 m, possibly caused by a deepening of the planetary boundary layer at the maximum of daytime heating (Miller 2012).

This snowfall event (classified as a Miller A/B) had far less substantial snowfall totals than Sandy due to the absence of unique synoptic scale forcing and antecedent air trajectories originating from the Atlantic Ocean. The storm also featured westerly-originating trajectories, compared to those with maritime trajectories from the north and east observed in Sandy's remnants. Additionally, the echo top heights and intensity were lower for this system as observed by the nearby MRR (<2200 m) due to the lack of substantial synoptic influence, especially during the latter portion of the storm. The contrast between these 2 events serves as an excellent example of the variety of synoptic influences in the SAM region.

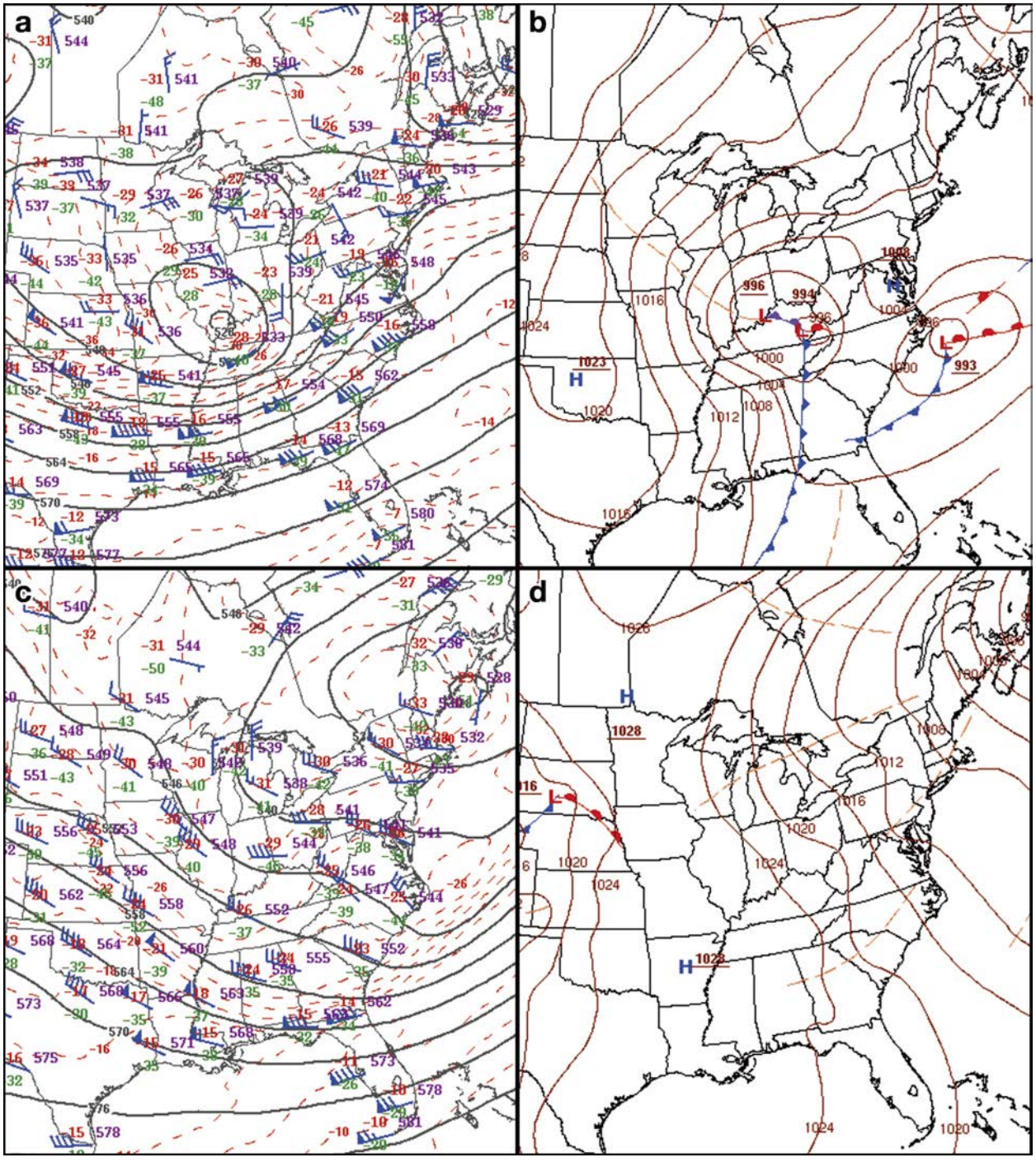

Fig. 10. NOAA Weather Prediction Center (WPC)-analyzed 500 hPa geopotential height (solid lines, dm), wind barbs (knots; 1 knot = 0.51 m s^{-1}) and temperature (°C, dashed lines) for the late March case study (a) 00:00 h UTC on 25 March 2013 and (c) 00:00 h UTC on 27 March, and (d) WPC surface analysis for the same times (data source: www.hpc.ncep.noaa.gov/html/sfc2.shtml). Colors as in Fig. 7

5. DISCUSSION

We characterized wind directions at Roan Mountain and nearby sites with a dominance (>70%) in northwest winds during snow events, which compares well with the 88% from previous studies that have analyzed this parameter (Perry & Konrad 2006, Perry et al. 2007, 2010, 2013). Despite this similarity in wind

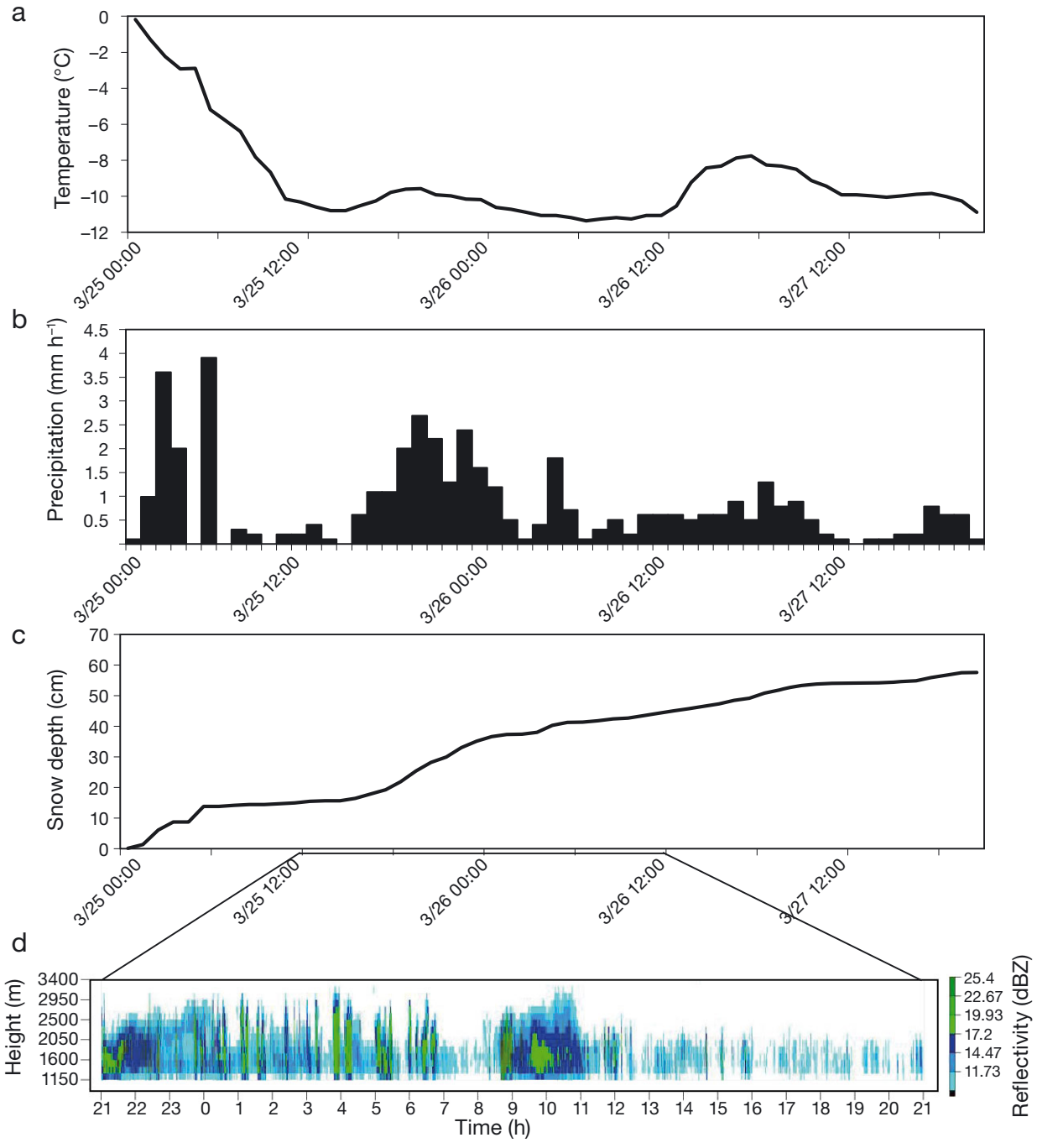

Fig. 11. (a) Hourly precipitation, (b) temperature, (c) cumulative snow depth, and (d) radar reflectivity for the 24 h period ending at 12:00 h UTC on 26 March 2013 for a late-March snow event. Radar reflectivity images (d) created using NCSU (North Carolina State University) OPL Micro Rain Radar application version 0.9.0.75 (Prerelease), North Carolina State University Department of Marine, Earth and Atmospheric Cloud and Sciences Precipitation Processes and Patterns Group

climatology, however, a dramatic difference in snowfall distribution from normal was seen this season. While favored upslope locations such as Boone and Mt. LeConte observed up to 81 and 124% of their average annual snowfall (88 and 324 cm, respectively), valley locations not commonly affected by NWFS saw totals well below the annual average; for example, Asheville received only 1 cm (8% of average annual snowfall) during the 2012–2013 season compared to an average annual snowfall of 30 cm. This lack of snowfall demonstrates the high spatial variability of NWFS events, while the lack of easterly flow due to

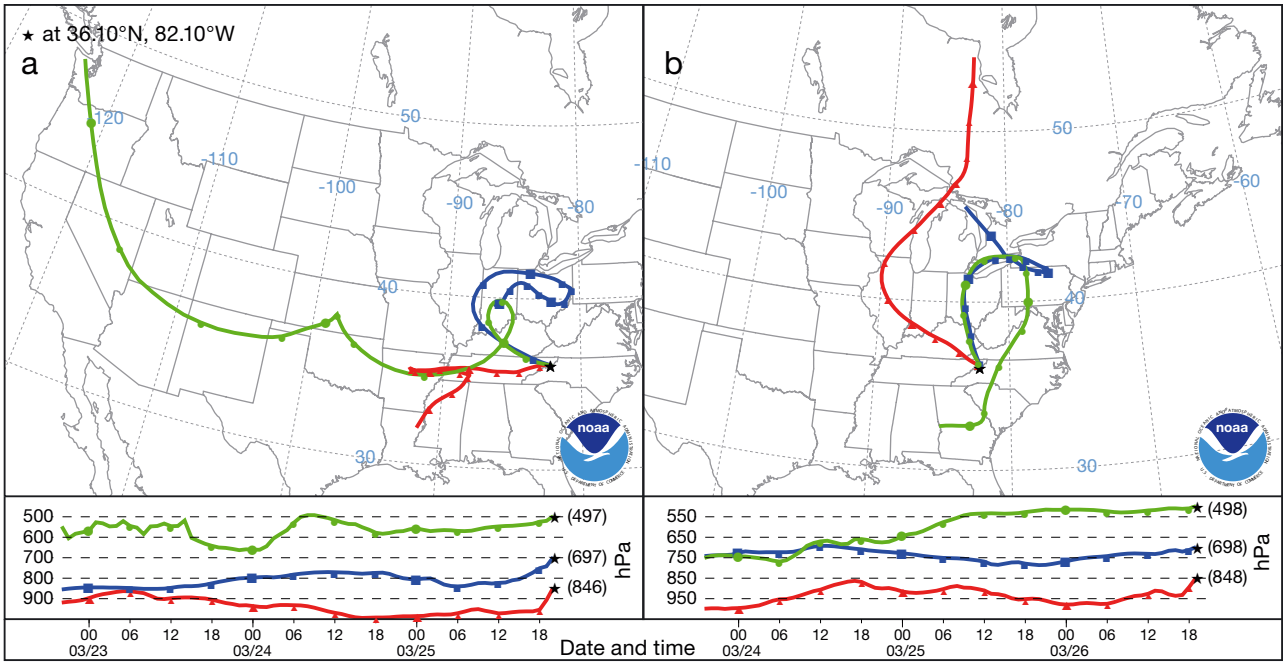

Fig. 12. 72 h backward HYSPLIT trajectory plots for mid-March ending at event hourly precipitation maxima. (a) 20:00 h UTC on 25 March 2013, (b) 19:00 h UTC on 26 March 2013. Red, blue and green lines represent backward parcels ending at Roan Mountain (starred) at approximately 850, 700, and 500 hPa, respectively. Values in parentheses: pressure of the air parcel at the end of its trajectory

fewer Miller-type systems highlights the importance of easterly or southerly flow for precipitation in areas of the SAM not heavily influenced by northwest flow snowfall (i.e. valley regions).

Roan Mountain received a substantial amount of forcing from NWFS, but it also saw snowfall from easterly and southerly flow, even if to a somewhat lesser extent than Mt. Mitchell. Peaks with a high prominence (e.g. Roan Mountain, Mt. LeConte) tend to not be dependent on any one synoptic regime for their seasonal snowfall, and therefore are less susceptible to inter-seasonal variation of snowfall totals as synoptic patterns vary (Perry et al. 2010). As such, Mt. Mitchell saw close to its average annual 230 cm (284 cm recorded), suggesting that while the mountain lacks similar northwest exposure, its prominence and elevation, like Roan Mountain's, allows for a lack of dependence on a single synoptic flow regime.

In snow seasons such as 2012–2013, higher elevations may still receive substantial snowfall due to favorable orographic effects even in the absence of synoptic patterns favoring the development of Miller cyclones. Regardless of location, the influence of elevation and exposure to wind directions typically seen in SAM upslope snow events (i.e. west–northwest) heavily dictates annual snowfalls observed in this highly variable spatial domain (Perry & Konrad 2006). As a major component of orographic precipitation processes, the knowledge of wind direction characteristics and climatology allows the identification of the most likely placement of precipitation maxima not only for the SAM, but also for other mountain regions (Basist et al. 1994).

Freezing rain was quite common in our dataset as well, with over 35 d where precipitation was recorded with sub-freezing temperatures and no snowfall accumulation. This value greatly exceeds coarser data analyses (e.g. Changnon & Karl 2003), which place maximum freezing rain days in the region on the order of 10–15. Due to a lack of a present weather sensor for a majority of the time, however, it is difficult to tell how much of this precipitation may have fallen as sleet or other mixed types not easily accumulated; nonetheless, it suggests freezing rain is a very common occurrence at the highest elevations of the SAM. The high frequency of freezing rain may also relate to the relatively low elevations of the highest peaks (<2037 m) in the SAM, resulting in orographic clouds with insufficiently low temperatures for ice nucleation.

Radar characteristics of snowfall events closely matched the distribution for a dataset collected from 2006–2009 (Perry et al. 2013). Although there is a strong synoptic dependence, melting layer heights

typically fell over the course of the event, suggesting that the most substantial cold air advection in the lower troposphere occurs before an event matures. Echo top heights also exhibited a reduction over the course of the event, suggesting that the characteristic low-level flow associated with NWFS events does not develop until after a bulk of the liquid precipitation amount has fallen and the synoptic-scale ascent has departed. This echo top height decrease is likely caused by synoptic-scale subsidence coincident with a capping inversion overtaking the area (Keighton et al. 2009). The very low echo top heights (<2500 m) for many of the NWFS events suggest that snow particles must grow rapidly within the shallow cloud layer, possibly in conjunction with horizontal convective rolls (e.g. Schultz et al. 2004) and/or rapid riming in the presence of abundant cloud liquid water.

Lapse rates are important to consider for diagnosing and forecasting snow events, particularly NWFS, as precipitation amounts can in part be driven by convective instability in the absence of synoptic-scale ascent (Miller 2012). While we would expect steep low-level lapse rates due to many storms being associated with lower and middle tropospheric cold air advection, a few events had low or even inverted lapse rates. This observation further indicates the likelihood of a CAD-style scenario being in place when these wind regimes are present (Bell & Bosart 1988). On average, events with higher lapse rates had similar amounts of liquid precipitation when compared with the remainder of the sample, which suggests that convective activity on average was not a dominant contributor to the observed snowfalls at the event scale. However, it should be noted that although embedded convection can cause greatly enhanced hourly snowfall rates (Miller 2012), one snow season may not have been sufficient to provide an adequate sample for statistical analysis. Nonetheless, the instability and high snowfall rates observed in the SAM are somewhat comparable to lake-effect snow in the Great Lakes, where convection embedded within snowstorms can yield exceptionally high snowfall amounts even with a shallow echo top height and in the presence of a strong subsidence inversion (Niziol et al. 1995, Holloway 2007). It should be noted, however, that a simple horizontal derivation of lapse rate has limitations, including but not limited to latent heating or cooling as clouds and precipitation form, locally strong cold air advection, and surface snow cover. Given our available datasets and the limitations of alternatives (e.g. low-resolution model reanalysis, a lack of nearby soundings), this *in situ* approach is best for gleaning vertical temperature gradients at the event level.

A lack of strong diurnal variation in precipitation distribution in the dataset is also worth noting. Previous work (Miller 2012) has suggested that daytime heating provides a complex contribution to snowfall by deepening the planetary boundary layer in such a way that snowfall totals could be minimized, but this effect may be negated by the increase in upstream water vapor by the latent heat flux. Given that the results suggest a relatively even distribution of precipitation overall by day (54%) and night (46%), it is possible that these mechanisms are balanced by each other, making nighttime totals not greatly different than those under daytime solar forcing. Additional data may be needed to further test this hypothesis.

The orographic enhancement factor allowed for a new perspective to be gained on the variability of precipitation change with elevation. Our findings on average were consistent with the orographic enhancement model proposed by Dore et al. (1992), although the magnitude of the observations for snowfall events was greater than those found in Scotland. This may be attributed to the surrounding subsidence common to synoptic regimes in the SAM which can squeeze the planetary boundary layer so that low-level parcels are not able to reach their lifting condensation level. Event-level observed enhancement values were also not uniform: the depth of moisture available likely drives whether a system's precipitation is relatively uniform (synoptically driven) or spatially inconsistent, being driven instead by local upslope/terrain effects. This lack in consistency may undermine the usefulness of traditional regression models (e.g. Daly et al. 2008) in the SAM, especially during mesoscale-driven events. While other studies (e.g. Perry & Konrad 2006) have refined these multivariate regression approaches for NWFS in the SAM, error still remains in statistical approaches, justifying the need to understand precipitation:elevation ratios as a function of more than just elevation or exposure. Nonetheless, development of a climatological orographic enhancement value for snow events based on different wind directions and synoptic classes would be a valuable metric for forecasters, hydrologists, and snow scientists in the SAM and other mountain regions.

6. CONCLUSIONS

The installation of the MOPRAM station at a high-elevation site favorable for substantial snowfall has allowed us to begin the development of a unique climatological dataset. Key findings to date include:

(1) Roan Mountain is likely the snowiest location in the SAM region, with total snowfall and SWE during the 2012–2013 snow season higher than at other observing stations on Mt. Mitchell and Mt. LeConte. (2) Significant seasonal snowfall may occur at higher elevations in the SAM even when valley locations experience a snow drought — this has hydrological implications, as a deep snowpack with high SWE can still develop in years that do not favor major snowstorms. (3) The majority of the snowfall at Roan Mountain and in the SAM occurs in association with west and northwest low-level flow and shallow echo tops. (4) Orographic enhancement of snowfall can be substantial (approaching 3.5:1 in some events) during periods of high moisture content and strong upslope flow, such as experienced during Sandy in October 2012.

Our findings also indicate patterns that meteorologists can seek when forecasting heavy orographic snowfall events. While the effects of elevation and exposure have been previously considered and surveyed (Perry & Konrad 2006), further expansion of this concept is explored in this work with the usage of local metrics such as observed orographic enhancement factors, which we have found can range up to a factor of 3 assuming similar exposure to upslope winds. Additionally, knowledge of NWFS cloud depth climatology from the use of vertically pointing radar can be used in conjunction with current WSR-88Ds experience to place where snowfall is occurring, even if not easily seen at more distant sites from the radar. Wind direction and synoptic event type are also important to consider, with Miller-style events with long durations of northwest flow contributing the most snowfall in typical NWFS-affected areas. However, exceptions to this rule exist — the highest elevation sites appear not as dependent on synoptic type for high snowfall accumulations as valley locations.

As the event database from this unique station grows, future climatological studies testing hypotheses about orographic snowfall processes can continue; the addition of Roan Mountain to the existing suite of monitoring stations will bolster the sampling availability for future research. The SAM region lacks a high sample size of stations at the crest of mountains, especially those on favorable NWFS escarpments. In this study, we explored in greater detail known driving factors behind substantial SWE amounts in the SAM (e.g. wind speed and direction, upstream lapse rates, antecedent air parcel trajectories) in greater detail. Valuable data such as the historic remains of Hurricane Sandy can be used in future in-depth case studies. Additionally, natural disasters can be caused by the nearly continuous nature of the snow cover. The ability to quantify high amounts of snow cover highlights potential hazards from heavy rain falls on existing snowpack.

Despite the uniqueness of this dataset, questions about the automated findings remain. This project has shown the value of such a database and the need for its collection to continue. If possible, manual observations should supplement the collection. Intensive observation periods should be considered to validate the automated sensor data and other manually collected parameters, especially snow depth and derived lapse rates corroborated with actual nearby atmospheric soundings. Installing a wind sensor on-site would allow for the investigation of mesoscale vs. synoptic flow regimes. Considering synoptic event characteristics in comparison with other low-lying sites could determine climatological parameters playing substantial roles in different regions of the SAM. Results from future short- and long-term atmospheric studies using these high-elevation data can be applied not only by interests in the SAM, but also by other scientists investigating the physical patterns influencing orographic precipitation. These findings can be transferred to mountain regions with similar topographic characteristics to improve the knowledge of orographic processes and improve the ability of forecasters to save lives and property.

Acknowledgements. We thank Mike Hughes, Dana Greene, and the Appalachian State University College of Arts and Sciences, as well as the Office of Student Research. We also recognize Dr. Sandra Yuter of North Carolina State University, as well as the Andrew Martin, Corey Davis, and others at the North Carolina State Climate Office. Jonathan Welker assisted with site installation. Steve Keighton and Laurence Lee assisted with synoptic event classification. We are also grateful for the comments from 3 anonymous reviewers. Material is based upon work supported by the National Science Foundation under Grant no. EAR 0949263.

LITERATURE CITED

Alcott TI, Steenburgh WJ (2013) Orographic influences on a Great Salt Lake-effect snowstorm. Mon Weather Rev 141:2432–2450

Barry RG (2008) Mountain weather and climate. Cambridge University Press, Cambridge

Basist A, Bell GD, Meentemeyer V (1994) Statistical relationships between topography and precipitation patterns. J Clim 7:1305–1315

Bell GD, Bosart LF (1988) Appalachian cold-air damming. Mon Weather Rev 116:137–161

Changnon SA, Karl TR (2003) Temporal and spatial variations of freezing rain in the contiguous United States: 1948–2000. J Appl Meteorol 42:1302–1315

Cifelli R, Doesken N, Kennedy P, Carey LD, Rutledge SA, Gimmestad C, Depue T (2005) The community collabora-

tive rain, hail, and snow network. Bull Am Meteorol Soc 86:1069–1077

Daly C, Halbleib M, Smith JI, Gibson WP and others (2008) Physiographically sensitive mapping of climatological temperature and precipitation across the conterminous United States. Int J Climatol 28:2031–2064

Doesken NJ (2007) Let it rain: how one grassroots effort brought weather into America's backyards. Weatherwise 60:50–55

Doesken NJ, Leffler RJ (2000) Snow foolin': accurately measuring snow is an inexact but important science. Weatherwise 53:31–37

Dore AJ, Choularton TW, Fowler D, Crossley A (1992) Orographic enhancement of snowfall. Environ Pollut 75: 175–179

Draxler RR, Rolph GD (1998) An overview of the HYSPLIT_4 modeling system of trajectories, dispersion, and deposition. Aust Meteorol Mag 47:295–308

Galarneau TJ, Davis CA, Shapiro MA (2013) Intensification of Hurricane Sandy (2012) through extratropical warm core seclusion. Mon Weather Rev 141:4296–4321

Gauer P (1998) Blowing and drifting snow in Alpine terrain: numerical simulation and related field measurements. Ann Glaciol 26:174–178

Hart RE, Evans JL (2001) A climatology of the extratropical transition of Atlantic tropical cyclones. J Clim 14:546–564

Holder C, Boyles R, Syed A, Niyogi D, Raman S (2006) Comparison of collocated automated (NCECONet) and manual (COOP) climate observations in North Carolina. J Atmos Ocean Technol 23:671–682

Holloway BS (2007) The role of the Great Lakes in northwest flow snowfall events in the southern Appalachian Mountains. MS thesis, North Carolina State University, Raleigh, NC

Hunter S, Boyd B (1999) Killer flooding in Carter County of extreme east Tennessee. National Weather Service. www.srh.noaa.gov/mrx/hydro/cflood/doeflood.php (accessed 03 Dec 2013).

Johnson R (1987) Southern snow: the winter guide to Dixie. Appalachian Mountain Club, Boston, MA

Keighton S, Lee L, Holloway B, Hotz D and others (2009) A collaborative approach to study northwest flow snow in the southern Appalachians. Bull Am Meteorol Soc 90: 979–991

Medina S, Smull F, Houze RA (2005) Cross-barrier flow during orographic precipitation events: results from MAP and IMPROVE. J Atmos Sci 62:3580–3598

Meyers M (2006) Power of the picturesque: motorists' perceptions of the Blue Ridge Parkway. Landscape 25:35–53

Miller DK (2012) Near-term effects of the lower atmosphere in simulated northwest flow snowfall forced over the Southern Appalachians. Weather Forecast 27:1198–1216

Miller JE (1946) Cyclogenesis in the Atlantic Coastal region of the United States. J Meteorol 3:31–44

National Park Service (2012) Monthly public usage report. https://irma.nps.gov/Stats/SSRSReports/Park Specific Reports/Monthly Public Use?RptDate=12/1/2012&Par=BLRI (accessed 11 December 2013)

NCSU (North Carolina State University) (2014) OPL Micro Rain Radar application version 0.9.0.75 (Prerelease). North Carolina State University Department of Marine, Earth and Atmospheric Sciences Cloud and Precipitation Processes and Patterns Group

Niziol TA, Snyder WR, Waldstreicher JS (1995) Winter weather forecasting throughout the eastern United States. IV. Lake effect snow. Weather Forecast 10:61–77

Perry LB (2006) Synoptic climatology of northwest flow snowfall in the southern Appalachians. PhD dissertation, University of North Carolina at Chapel Hill, NC

Perry LB, Konrad CE (2006) Relationships between NW flow snowfall and topography in the Southern Appalachians, USA. Clim Res 32:35–47

Perry LB, Konrad CE, Schmidlin TW (2007) Antecedent air trajectories associated with northwest flow snowfall in the Southern Appalachians. Weather Forecast 22: 334–352

Perry LB, Konrad CE, Hotz DG, Lee LG (2010) Synoptic classification of snowfall events in the Great Smoky Mountains, USA. Phys Geogr 31:156–171

Perry LB, Keighton SJ, Lee LG, Miller DK, Yuter SE, Konrad CE (2013) Synoptic influences on snowfall event characteristics in the southern Appalachian Mountains. Langlois A, Frankenstein S (eds) Proc 70th Annu East Snow Conf, 4–6 June 2013, Huntsville, ON, Canada, p 141–157

Peters G, Fischer B, Andersson T (2002) Rain observations with a vertically looking Micro Rain Radar (MRR). Boreal Environ Res 7:353–362

Rasmussen R, Baker B, Kochendorfer J, Meyers T, Landolt S and others (2012) How well are we measuring snow? The NOAA/FAA/NCAR winter precipitation test bed. Bull Am Meteorol Soc 93:811–829

Ryan WA, Doesken NJ, Fassnacht SR (2008) Evaluation of ultrasonic snow depth sensors for U.S. snow measurements. J Atmos Ocean Technol 25:667–684

Schultz DM, Arndt DS, Stensrud DJ, Hanna JW (2004) Picture of the month: snowbands during the cold-air outbreak of 23 January 2003. Mon Weather Rev 132: 827–842

Sevruk B, Ondras M, Chivila B (2009) The WMO precipitation measurement intercomparisons. Atmos Res 92:376–380

Stark D, Colle BA, Yuter SE (2013) Observed microphysical evolution of the two East Cboast winter storms and the associated snow bands. Mon Weather Rev 141:2037–2057

Wooten RM, Gillon KA, Witt AC, Latham RS and others (2008) Geologic, geomorphic, and meteorological aspects of debris flows triggered by Hurricanes Frances and Ivan during September 2004 in the Southern Appalachian Mountains of Macon County, North Carolina (southeastern USA). Landslides 5:31–44

Yuter SE, Kingsmill DE, Nance LB, Loffler-Mang M (2006) Observations of precipitation size and fall speed characteristics within coexisting rain and wet snow. J Appl Meteorol 45:1450–1464

Yuter SE, Stark DA, Bryant MT, Colle BA and others (2008) Forecasting and characterization of mixed precipitation events using the MicroRainRadar. Proc 5th European Conf on Radar Meteorol and Hydrol. 30 June–4 July 2008, Helsinki

Editorial responsibility: Oliver Frauenfeld, College Station, Texas, USA

Submitted: February 10, 2014; Accepted: January 27, 2015 Proofs received from author(s): May 1, 2015